

# Monoclonal Antibody AE-2 Modulates Carbamate and Organophosphate Inhibition of Fetal Bovine Serum Acetylcholinesterase

A. D. WOLFE, P. K. CHIANG, B. P. DOCTOR, N. FRYAR, J. P. RHEE, and M. SAEED

Division of Biochemistry, Walter Reed Army Institute of Research, Washington, D. C. 20307-5100

Received March 8, 1993; Accepted September 11, 1993

Downloaded from molpharm.aspetjournals.org at Thammasart University on December 3, 2012

## SUMMARY

The monoclonal antibody AE-2, raised against the human erythrocyte acetylcholinesterase (AChE) dimer (acetylcholine acetylhydrolase, EC 3.1.1.7), binds to other mammalian AChEs, including the tetramer that occurs in fetal bovine serum (FBS). AE-2 partially inhibited the rate of hydrolysis of the charged substrate acetylthiocholine by FBS AChE, whereas it increased the rate of hydrolysis of the neutral substrate indophenyl acetate. Present

results show that AE-2 decreases the rate of inhibition of FBS AChE by the positively charged organophosphate amiton-*p*-toluene sulfonate and the positively charged carbamates pyridostigmine and neostigmine but accelerates inhibition of FBS AChE by the neutral organophosphates paraoxon and diisopropylfluorophosphate. Results suggest that AE-2 may allosterically modulate an anionic site in the catalytic center of FBS AChE.

The mAb AE-2 was raised (1) against the human erythrocyte AChE dimer but binds to and partially inhibits AChEs from adult and fetal human brain tissue (2) and from FBS (3-5). It also binds to but does not inhibit (5) TcAChE (6). AE-2 is a conformational antibody (2, 5) that inhibits FBS AChE hydrolysis of ATC (2, 7) by 80% but increases IPA hydrolysis by 15-fold (7). Maximal decrease in ATC hydrolysis and maximal increase in IPA hydrolysis occur at a 4-fold molar excess of AE-2 with respect to enzyme active sites (2, 7). Both inhibition and acceleration are noncompetitive, with the respective  $K_m$  values for these processes remaining unchanged while their  $V_{max}$  values are altered (2, 7). AE-2 does not alter substrate inhibition (2), which has been reported to occur at the peripheral anionic site (8), but the equilibrium between AE-2 and AChE is perturbed (2, 7) by the active site ligands edrophonium and pralidoxime chloride, suggesting that the AE-2 epitope is related to the active center anionic site. We now report that AE-2 also modulates the rate of AChE inhibition by OPs and CBs, regardless of whether ATC or IPA is used as the substrate. Thus AE-2, complexed to FBS AChE, retards the rate of AChE inhibition by the positively charged inhibitors pyridostigmine, neostigmine, and amiton, whereas it increases the rate of inhibition by the uncharged OPs paraoxon and DFP. An analogous perturbation of activity occurs upon treatment of AChE with aziridinium ion-generating alkylating agents (9-11), or with protein-modifying reagents (12), whereas a cassette mutation (13) caused similar kinetic changes in the hydrolysis of ATC. Present results extend the findings with AE-2, ATC, and

IPA to positively charged and neutral OP and CBs, and they suggest allosteric AE-2 modulation of sites within the AChE gorge (14).

## Materials and Methods

FBS (GIBCO, Grand Island, NY) AChE was purified to homogeneity by procainamide affinity gel chromatography (15). Amiton-*p*-toluene sulfonate was a gift of Donald M. Maxwell, United States Army Medical Research Institute of Chemical Defense (Aberdeen Proving Ground, Aberdeen, MD). Pyridostigmine, neostigmine, DFP, paraoxon, ATC, and IPA were purchased from Sigma Chemical Co. (St. Louis, MO).

The activity of FBS AChE, free or complexed with AE-2, was assayed colorimetrically (16) using a concentration of 1 mM ATC as substrate, in a volume of 3.0 ml of 0.1 M phosphate buffer, pH 8.0, containing  $3.11 \times 10^{-7}$  M 5,5'-dithio-bis(2-nitrobenzoic acid). One unit of FBS AChE activity is defined as the hydrolysis of 1  $\mu$ mol of 1 mM ATC/min at 25° in 0.1 M phosphate buffer, pH 8.0. Some experiments were also conducted with IPA as substrate (12). Such reaction systems contained a concentration of 0.5 mM IPA in 3.0 ml of 0.05 M phosphate buffer, pH 8.0, and were assayed at a wavelength of 625 nm (12). All reactions were conducted at 25°. Typical incubations for the formation of AE-2-FBS AChE complexes were conducted for 18 hr in 0.05 M phosphate buffer, pH 8.0, and contained  $3.8 \times 10^{-8}$  M to  $1.7 \times 10^{-7}$  M FBS AChE active sites and a 6-28-fold molar excess of AE-2. AChE concentrations are presented in terms of enzyme active sites; ratios of AE-2 to AChE are presented in terms of multiples of AE-2 required (2, 7) to saturate AChE (4/1); thus, a 6/1 AE-2/AChE ratio is 1.5-fold saturation. The ATC-hydrolyzing activity of AE-2-FBS AChE com-

**ABBREVIATIONS:** AChE, acetylcholinesterase; FBS, fetal bovine serum; ATC, acetylthiocholine; TcAChE, *Torpedo californica* acetylcholinesterase; mAb, monoclonal antibody; IPA, indophenyl acetate; OP, organophosphate; CB, carbamate; DFP, diisopropylfluorophosphate.

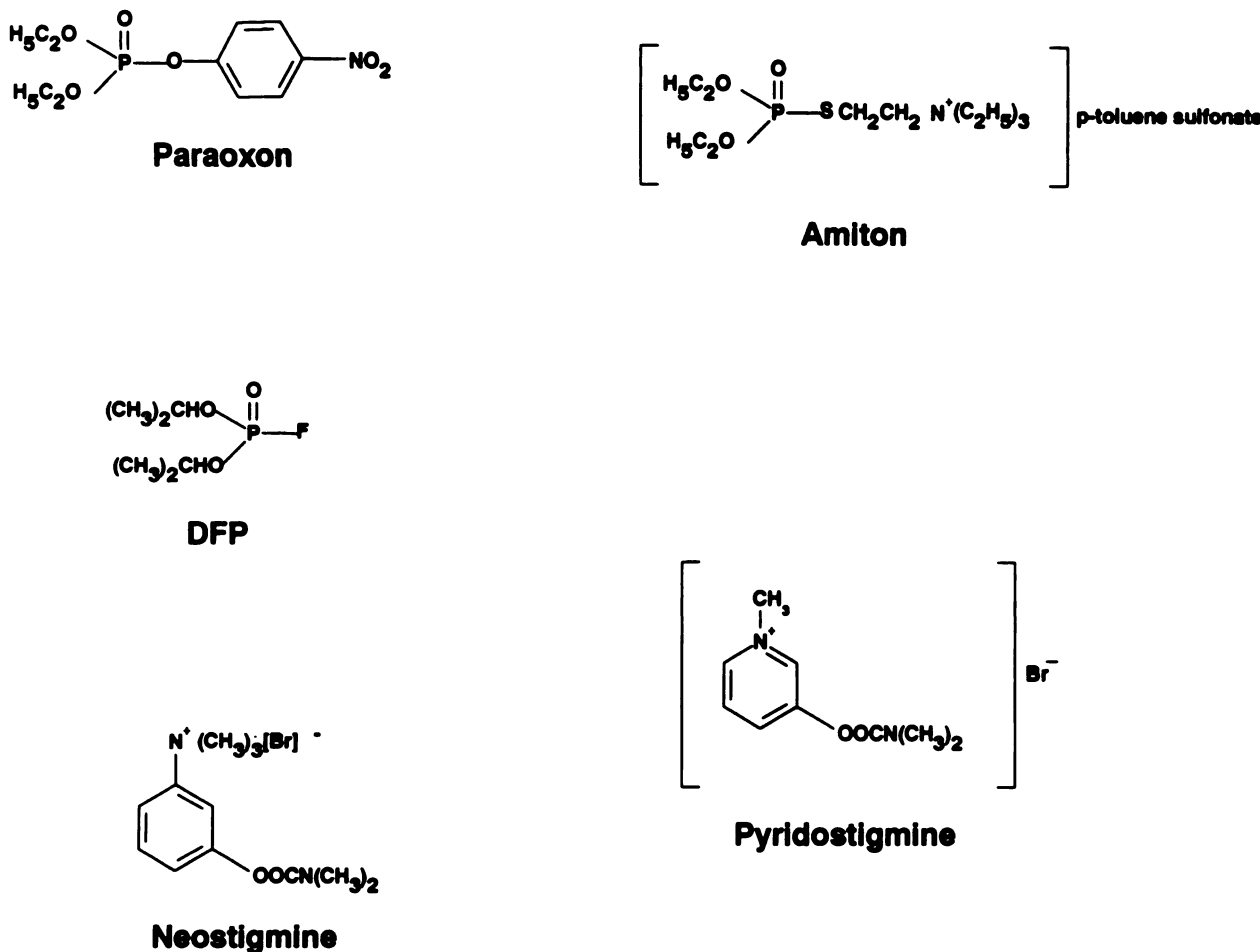
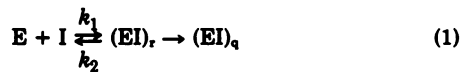


Fig. 1. Structures of the CBs and OPs used in these studies.

plexes was typically reduced to 25% that of the free enzyme, although during the 2-year course of these investigations AE-2 appeared to lose 10–15% of its inhibitory effect. For inhibition analysis, the initial volume of such mixtures varied from 600  $\mu$ l to 1000  $\mu$ l and was divided into 50- $\mu$ l or 100- $\mu$ l aliquots for use; graded concentrations of OP or CB were introduced into such mixtures, and 5- $\mu$ l or 10- $\mu$ l aliquots were withdrawn at time intervals for immediate assay. Enzyme or enzyme-antibody complexes were assayed for activity for a minimum of 30 sec, to establish an initial linear progress curve for analysis. A Varian DMS-200 spectrophotometer, driven by the program Spectracalc (Galactic Industries, Nashua, NH), was used in all experiments.

Eq. 1 (17) describes the reaction between OP or CBs and AChE:



where E and I are the enzyme and inhibitor concentrations, respectively,  $(EI)_r$  is the concentration of the enzyme-inhibitor intermediate, and  $(EI)_q$  is the concentration of the “irreversible” enzyme-inhibitor complex (17);  $K_e = k_2/k_1$  is the equilibrium dissociation constant for the initial reaction between inhibitor and enzyme. Eq. 2, derived from this reaction scheme, was used to analyze inhibition data graphically (17) to obtain the appropriate kinetic constants.

$$1/i = (\Delta t / 2.303 \Delta \log v) k_r - 1/K_e \quad (2)$$

In this equation,  $i$  is the inhibitor concentration,  $t$  is time in minutes, and  $v$  is reaction velocity. Pseudo-first-order inhibition curves were used to construct replots in which the slope is equal to the bimolecular rate constant  $k_r$ , the intercept on the ordinate ( $1/i$ -axis) is equal to  $-1/K_e$ ,

and the intercept on the  $x$ -axis is equal to  $1/k_p$  or  $1/k_c$ . The constant  $k_p$  is the phosphorylation constant and  $k_c$  is the carbamylation constant. These terms should obey the relationship  $k_c = k_p/K_e$  (17).

## Results

Paraoxon and DFP are OPs that lack a positive charge, in contrast to amiton and the CBs neostigmine and pyridostigmine (Fig. 1). Incubation of FBS AChE with paraoxon, in the absence and presence of AE-2, showed AE-2 to markedly accelerate paraoxon inhibition of the enzyme (Fig. 2, *upper*). In the presence of AE-2, a 2-fold ratio of paraoxon to complex was sufficient to cause complete enzyme inhibition in <4 min. In the absence of AE-2, this ratio of paraoxon to enzyme produced approximately 60% inhibition in 30 min. AE-2 caused a 5-fold (Fig. 2, *inset*; Table 1) increase in the bimolecular rate constant for paraoxon at inhibitor/enzyme ratios between 2 and 30, at a mAb/AChE ratio of 5 times saturation. Table 2 shows AE-2 to cause an 11-fold increase in the affinity ( $K_e$ ) of the enzyme for paraoxon, while simultaneously causing a 2-fold reduction ( $k_p$ ) in the phosphorylation rate. AE-2 also accelerated DFP inhibition of AChE (Fig. 2, *lower*; Table 1). Affinity and velocity data for DFP were unobtainable from this plot because the rate did not converge to a maximum value in the concentration range used. An identical result was obtained in the original paper (17) describing this form of graphical analysis.

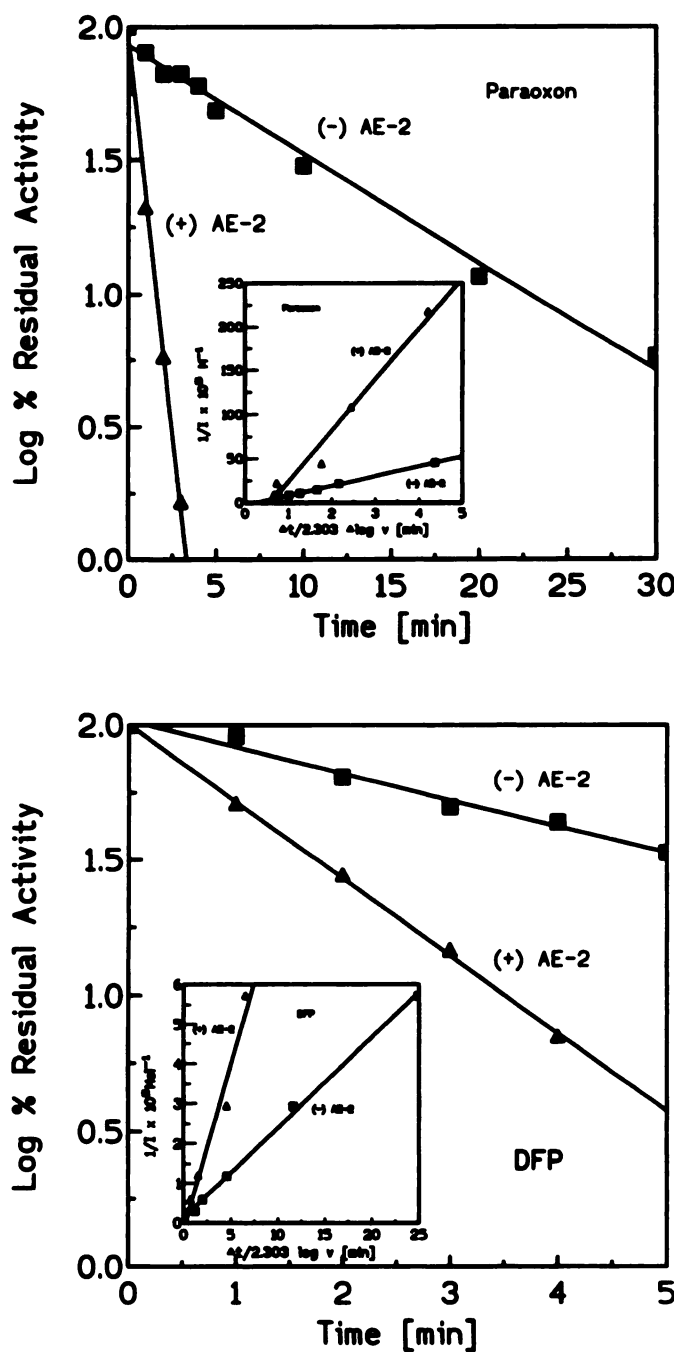


**Fig. 2.** Upper, pseudo-first-order plots of paraoxon inhibition of  $1.84 \times 10^{-7}$  M FBS AChE in the absence (■) and presence (▲) of a 3.75-fold saturating ratio of AE-2 to AChE active sites and a paraoxon concentration of  $3.59 \times 10^{-7}$  M. Inset, replots of the reciprocal of the slopes of pseudo-first-order reaction curves versus the reciprocal of the paraoxon concentrations, illustrating the acceleration of paraoxon inhibition by AE-2. The concentration of FBS AChE in both groups of reaction mixtures was  $3.97 \times 10^{-8}$  M (activity without AE-2, 15.6 units/ml; with AE-2, 5.3 units/ml). The concentrations of paraoxon for reaction mixtures lacking AE-2 were  $1.15 \times 10^{-6}$  M,  $9.2 \times 10^{-7}$  M,  $6.9 \times 10^{-7}$  M,  $4.62 \times 10^{-7}$  M, and  $2.3 \times 10^{-7}$  M; paraoxon concentrations in the AE-2-containing mixtures were  $1.15 \times 10^{-6}$  M,  $9.2 \times 10^{-7}$  M,  $3.7 \times 10^{-7}$  M,  $2.3 \times 10^{-7}$  M,  $9.2 \times 10^{-8}$  M, and  $4.62 \times 10^{-8}$  M. Ten-microliter aliquots were withdrawn every 30 sec for assay. Lower, typical pseudo-first-order plots and replots (inset) illustrating AE-2 acceleration of DFP inhibition of FBS AChE.

In contrast to the effects of AE-2 on paraoxon and DFP inhibition of AChE, AE-2 retarded amiton, pyridostigmine, and neostigmine inhibition of both ATC and IPA hydrolysis (Figs. 3 and 4; Tables 1 and 2). Inhibition of AE-2-AChE hydrolysis of ATC by amiton-*p*-toluene sulfonate contrasted strikingly with inhibition by paraoxon and DFP. Fig. 3 illustrates pseudo-first-order plots for inhibition of FBS AChE by amiton-*p*-toluene sulfonate in the absence and in the presence of AE-2; Fig. 3, inset, presents a replot that compares amiton inhibition of ATC hydrolysis by FBS AChE in the absence and in the presence of a saturating mAb/enzyme ratio of 7. AE-2 caused a 10-fold decrease in the rate of amiton inhibition (Table 1). The replot for amiton inhibition of free AChE also passed through the origin, therefore preventing a quantitative comparison between systems lacking and containing AE-2. AE-2 apparently increased the affinity of amiton for the complex but decreased the phosphorylation velocity.

Neostigmine and pyridostigmine inhibition of free FBS AChE and AE-2-FBS AChE complexes is depicted in Fig. 4, which illustrates typical pseudo-first-order reaction kinetics and replots using ATC as the substrate in the absence of AE-2 and both ATC and IPA (neostigmine replot) as substrates in the presence of a 5-fold saturating ratio of AE-2 to FBS AChE. Replots for neostigmine inhibition of AE-2-AChE could be presented as a single curve formed from results with both ATC and IPA (Fig. 4; Tables 1 and 2). AE-2 reduced both the

TABLE 1  
Summary of bimolecular rate constants

In view of the occasional use of low inhibitor to enzyme ratios, bimolecular rate constants were also routinely calculated (26) by means of appropriate integral equations for the hydrolysis of ATC, from the slopes of 10 or more pseudo-first-order plots produced for each inhibitor in the absence and presence of AE-2. All differences between systems containing or lacking AE-2 were significant at  $p < 0.001$ . When IPA was substituted for ATC, bimolecular rate constants for AE-2-AChE were similar to those obtained with ATC, except for amiton, which yielded a rate constant that was 10-fold lower than that listed.

Inhibitor	Rate constant		
	+AE-2 $\text{M}^{-1} \text{ min}^{-1}$	-AE-2 $\text{M}^{-1} \text{ min}^{-1}$	Ratio +/−
Neostigmine	$3.80 \times 10^5$	$1.96 \times 10^6$	0.19
Amiton	$1.18 \times 10^5$	$1.01 \times 10^6$	0.11
Pyridostigmine	$8.79 \times 10^4$	$2.29 \times 10^5$	0.38
Paraoxon	$5.79 \times 10^5$	$1.09 \times 10^6$	5.31
DFP	$8.20 \times 10^4$	$2.27 \times 10^4$	3.61

TABLE 2

Carbamylation ( $k_c$ ), phosphorylation ( $k_p$ ), and dissociation ( $K_d$ ) constants for inhibition of FBS AChE hydrolysis of ATC in the absence and presence of AE-2

Values were determined from appropriate intercepts (see Materials and Methods).

	$k_p$ or $k_c$			$K_d$		
	+AE-2 $\text{min}^{-1}$	-AE-2 $\text{min}^{-1}$	+/-	+AE-2 $\text{M}$	-AE-2 $\text{M}$	+/- $\text{M}$
Paraoxon	1.75	4.01	0.43	$3.29 \times 10^{-7}$	$3.76 \times 10^{-8}$	0.09
Pyridostigmine	1.73	4.95	0.34	$1.97 \times 10^{-5}$	$1.65 \times 10^{-6}$	1.19
Neostigmine	0.86	1.38	0.62	$2.05 \times 10^{-6}$	$7.09 \times 10^{-7}$	2.89

Experimental concentrations: FBS AChE,  $1.80 \times 10^{-7}$  M (activity without AE-2, 62.8 units/ml; with AE-2, 20.3 units/ml); 5-fold saturating ratio of AE-2 to FBS AChE;  $8.5 \times 10^{-6}$  M DFP. Inset, replots of pseudo-first-order kinetics for AE-2 acceleration of DFP inhibition of FBS AChE. DFP concentrations were  $3.4 \times 10^{-6}$  M,  $1.75 \times 10^{-6}$  M,  $8.5 \times 10^{-6}$  M,  $3.4 \times 10^{-6}$  M, and  $1.75 \times 10^{-6}$  M. Ten-microliter aliquots were withdrawn every 1 min for assay.

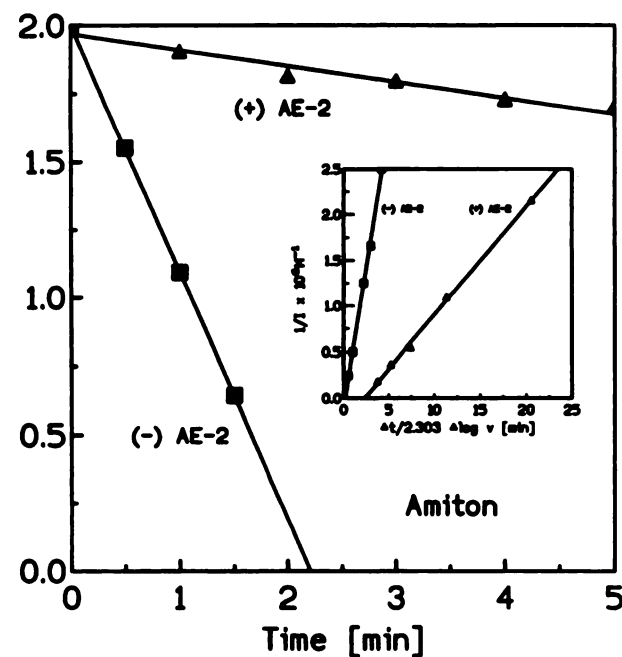


**Fig. 3.** Typical pseudo-first-order reaction plot, illustrating inhibition of FBS AChE by  $1.86 \times 10^{-6} \text{ M}$  amiton-*p*-toluene sulfonate in the absence (■) and in the presence (▲) of a 7-fold saturating ratio of AE-2 to FBS AChE. The original enzyme concentration was  $1.02 \times 10^{-7} \text{ M}$  (39.9 units/ml), and AE-2 reduced the ATC-hydrolyzing activity to 12.68 units/ml. *Inset*, replots of pseudo-first-order reaction kinetics were produced with the following concentrations of amiton:  $5.58 \times 10^{-6} \text{ M}$ ,  $2.79 \times 10^{-6} \text{ M}$ ,  $1.86 \times 10^{-6} \text{ M}$ ,  $9.11 \times 10^{-7} \text{ M}$ , and  $4.65 \times 10^{-7} \text{ M}$ . Five-microliter aliquots were withdrawn every 30 sec or 1 min, depending upon the amiton concentration, for assay.

carbamylation rate and the initial affinity of the enzyme for both neostigmine and pyridostigmine inhibition of FBS AChE (Table 2).

## Discussion

Previous work has shown that the mAb AE-2 partially inhibits the rate of hydrolysis of the charged ester ATC, while increasing the rate of hydrolysis of the neutral ester IPA (7). Present research extends these findings to show that AE-2 slows inhibition of FBS AChE by the protonated OP and CB inhibitors amiton, neostigmine, and pyridostigmine and accelerates inhibition by the neutral OP inhibitors paraoxon and DFP. In instances where the bimolecular step is not rate limiting and a non-zero intercept on the graph could be ascertained (paraoxon, pyridostigmine, and neostigmine) (Table 2), AE-2 reduced both the velocity constant and the affinity of the CBs and amiton for the complex, as opposed to the free enzyme. The affinity of the complex, as opposed to the enzyme, increased by a factor of 11 for paraoxon, suggesting that AE-2 either was increasing the efficiency of a site to which paraoxon bound or was neutralizing a site that negatively influenced its binding. It is noteworthy, however, that the magnitude of the phosphorylation constant for paraoxon decreased to a similar extent as did the carbamylation constants, despite the overall differences in the rates of inhibition. These results differ from those obtained with ATC and IPA (7) in that AE-2 did not change the affinity ( $K_m$ ) of FBS AChE for the respective substrates but reduced the  $V_{max}$  for the charged substrate ATC and increased the  $V_{max}$  for the neutral substrate IPA. Thus, it

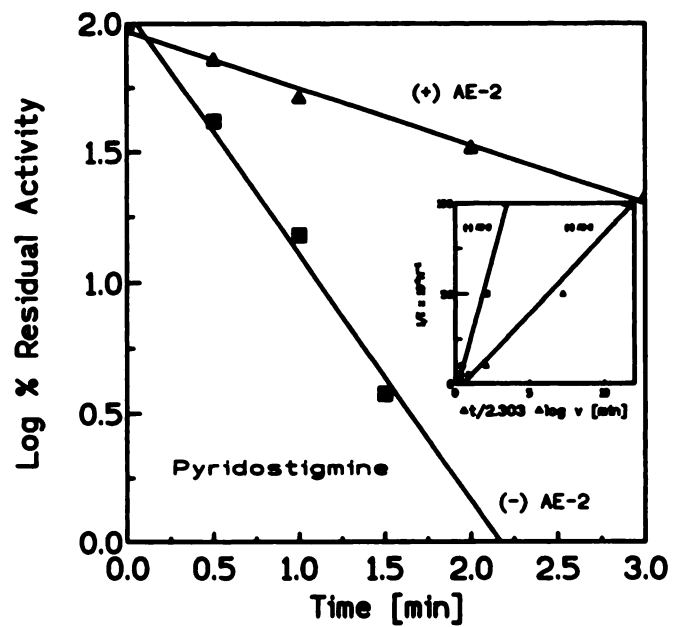
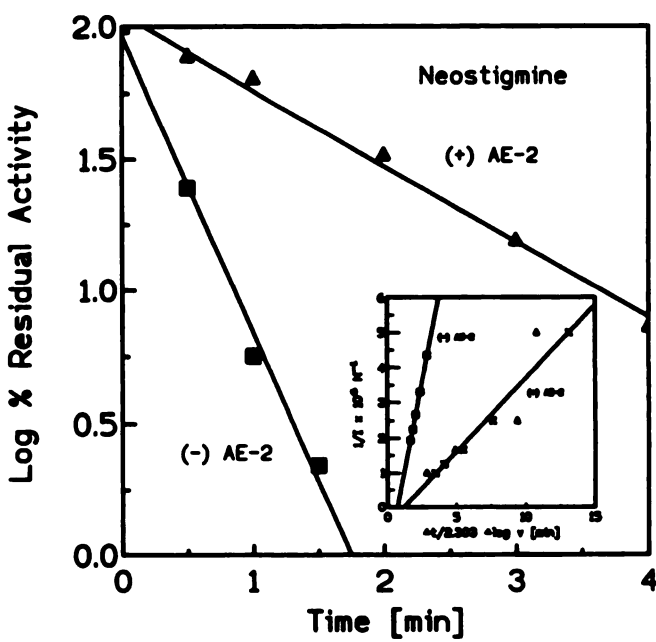


**Fig. 4.** Upper, pseudo-first-order plots of AE-2 retardation of  $2 \times 10^{-6} \text{ M}$  neostigmine inhibition of ATC hydrolysis by  $1.01 \times 10^{-7} \text{ M}$  FBS AChE, and replots (*inset*) comparing concentration versus pseudo-first-order slope reciprocals, in which AE-2 systems contained either ATC or IPA. In replots: FBS AChE without AE-2,  $5.97 \times 10^{-6} \text{ M}$  (23.5 units/ml); FBS AChE with AE-2,  $1.78 \times 10^{-6} \text{ M}$ ; activity, 30.2 units/ml (5-fold saturating ratio of AE-2). Neostigmine concentrations: ■ (AChE plus ATC),  $5.15 \times 10^{-7} \text{ M}$ ,  $4.46 \times 10^{-7} \text{ M}$ ,  $3.75 \times 10^{-7} \text{ M}$ ,  $3.03 \times 10^{-7} \text{ M}$ , and  $2.3 \times 10^{-7} \text{ M}$ ; ▲ (AE-2-AChE plus ATC),  $3.88 \times 10^{-6} \text{ M}$ ,  $3.43 \times 10^{-6} \text{ M}$ ,  $2.97 \times 10^{-6} \text{ M}$ ,  $2.50 \times 10^{-6} \text{ M}$ ,  $2.02 \times 10^{-6} \text{ M}$ , and  $1.84 \times 10^{-6} \text{ M}$ ; × (AE-2 plus IPA),  $9.09 \times 10^{-7} \text{ M}$ ,  $7.41 \times 10^{-7} \text{ M}$ ,  $5.86 \times 10^{-7} \text{ M}$ ,  $3.85 \times 10^{-7} \text{ M}$ , and  $1.96 \times 10^{-7} \text{ M}$ . With ATC, 10- $\mu$ l aliquots were withdrawn every 1 min for assay; with IPA, 10- $\mu$ l aliquots were withdrawn every 2 min for assay. Substitution of IPA for ATC did not change the bimolecular rate constant for neostigmine with AE-2-FBS AChE ( $r^2 = 0.90$  for this replot). Lower, pseudo-first-order plots of  $1 \times 10^{-6} \text{ M}$  pyridostigmine inhibition of the hydrolysis of ATC by  $9.97 \times 10^{-6} \text{ M}$  FBS AChE (■ (without AE-2), 39.9

appears that, whereas AE-2 differentially modulates the reaction of AChE with protonated in contrast to neutral substrates and hemi-substrates (inhibitors), qualitative differences occur between the dissociation and rate constant terms that *in toto* comprise catalysis or inhibition. In addition, limited experiments that compared OP and CB inhibition of IPA and ATC hydrolysis suggested that the two substrates were processed by similar catalytic mechanisms and inhibited at the same site.

Although the epitope for AE-2 is unknown, a CNBr-cleaved peptide consisting of FBS AChE amino acids 53–84 (5) competed with AE-2 for binding to FBS AChE, suggesting that this sequence contains one of the AE-2 binding regions. Dot blot enzyme-linked immunosorbent assays (5) also showed AE-2 to bind to the analogous sequence from TcAChE, but AE-2 was not inhibitory. Approximately 50% homology occurs between these enzymes in this sequence (4, 6). In addition, the mAbs 4E7 and 2C9, raised against TcAChE, also bind to residues within this sequence but do not inhibit TcAChE (18). The 2C9 epitope has been identified as the sequence 47–63 (18). This sequence lies on the surface of the enzyme, as a portion of the hairpin loop before the first  $\alpha$ -helix. In contrast, the putative AE-2 binding region extends beyond position 63 to FBS AChE position 84 and contains one amino acid recognized to possess unusual catalytic significance [ $D_{74}$  in human AChE (19) and FBS AChE (4),  $D_{72}$  in TcAChE (6), and  $D_{70}$  in butyrylcholinesterase (20)]. However, AE-2 fails to inhibit butyrylcholinesterase, and cassette mutations (13, 21) of  $D_{74}$  produce a considerable increase in  $K_m$  values while minimally reducing  $k_{cat}$ .

Crystallographical analysis (14) of TcAChE shows  $W_{84}$  to be a portion of the anionic site at the active center of AChE, binding the quaternary ammonium substituents of acetylcholine and edrophonium at the base of the gorge, proximal to the catalytic center  $S_{300}$  (6, 14). It was speculated (14) that neostigmine, a carbamyl analog of edrophonium and one of the inhibitors used in the present studies, may be expected to be positioned similarly to edrophonium. High concentrations of edrophonium, as well as pralidoxime chloride, tend to drive the AE-2/AChE equilibrium towards dissociation (2, 7). Edrophonium also caused reorientation of the gorge constituent  $F_{330}$  (FBS AChE  $Y_{337}$ ). Mutation of human AChE  $Y_{337A}$  produced the kinetic characteristics of AE-2-FBS AChE, in that it caused a 75% reduction in the  $V_{max}$  of ATC, whereas the  $K_m$  remained unchanged. Thus, some data suggest that AE-2 perturbs either  $W_{84}$  or  $Y_{337}$ , or both, most probably through an allosteric mechanism, in view of the dimensions of the AChE gorge. The length of the peptide competing with AE-2 may also be significant, however, because this peptide terminates only two amino acids short of FBS AChE  $W_{84}$ .

Chemical treatment of AChE also produced effects similar to those of AE-2 binding to FBS AChE. Thus,  $W_{84}$  was one of several alkylation sites (22, 23) in TcAChE. Alkylation of bovine erythrocyte AChE (11) resulted in a decrease in  $V_{max}$  for ATC and an increase in  $V_{max}$  for IPA. Their respective  $K_m$  values remained constant. Alkylation of bovine erythrocyte AChE also produced a larger reduction in the bimolecular rate

units/ml;  $\Delta$  (with AE-2), 5-fold saturation = 14.54 units/ml]. Inset, replot of the slopes of these and additional curves. FBS AChE and AE-2 concentrations were as described above. Pyridostigmine concentrations:  $5 \times 10^{-6}$  M,  $2 \times 10^{-6}$  M,  $1 \times 10^{-6}$  M,  $2 \times 10^{-6}$  M, and  $1 \times 10^{-6}$  M. Five-microliter aliquots were withdrawn every 20 or 30 sec, depending upon the pyridostigmine concentration, and were assayed immediately.

constant for protonated inhibitors than for paraoxon (11); indeed, the rate constant for amiton was decreased approximately 900-fold. It also appeared, however, that sulfur-containing OPs were more severely affected than was paraoxon (11). Alkylation also perturbed the peripheral anionic site (9–11, 22, 23), and incubation of alkylated eel AChE with curare resulted in inhibition of IPA hydrolysis. AE-2 did not appear to alter  $K_m$ , the substrate inhibititon constant, however (2). Treatment of bovine erythrocyte AChE with *N*-bromosuccinimide, which specifically binds to or alters tyrosine, tryptophan, and thiol groups, resulted in similar effects on ATC and IPA hydrolysis. Among the basis for the effects of chemical treatment of AChE appears to be perturbation or alteration of TcAChE  $W_{84}$  (FBS AChE and human AChE  $W_{186}$ ) and TcAChE  $F_{330}$  (human AChE and FBS AChE  $Y_{337}$ ). Parallel effects result from specific chemical treatment and AE-2 binding and appear to reinforce the inference that AE-2 allosterically perturbs either  $W_{84}$  or  $Y_{337}$ , or both.

#### Acknowledgments

The authors are pleased to acknowledge helpful discussions with Dr. Yacov Ashani.

#### References

1. Fambrough, D. M., A. G. Engel, and T. L. Rosenberry. Acetylcholinesterase of human erythrocytes and neuromuscular junctions: homologies revealed by monoclonal antibodies. *Proc. Natl. Acad. Sci. USA* **79**:1078–1082 (1982).
2. Sorensen, K., U. Brodbeck, A. G. Rasmussen, and B. Norgaard-Pedersen. An inhibitory antibody to human acetylcholinesterase. *Biochim. Biophys. Acta* **912**:56–65 (1987).
3. Ralston, J. S., R. S. Rush, B. P. Doctor, and A. D. Wolfe. Acetylcholinesterase of fetal bovine serum. *J. Biol. Chem.* **260**:4312–4318 (1985).
4. Doctor, B. P., T. C. Chapman, C. E. Christner, C. D. Deal, D. M. De La Hoz, M. K. Gentry, R. A. Ogert, R. S. Rush, K. K. Smyth, and A. D. Wolfe. Complete amino acid sequence of fetal bovine serum acetylcholinesterase and its comparison in various regions with other cholinesterases. *FEBS Lett.* **266**:123–127 (1990).
5. Doctor, B. P., K. K. Smyth, M. K. Gentry, R. A. Ogert, and S. W. Smith. Structural and immunocchemical properties of fetal bovine serum acetylcholinesterase, in *Progress in Clinical and Biological Research*, Vol. 289 (R. Rein and A. Golumbeck, eds.). Alan R. Liss, Inc., New York, 305–316 (1989).
6. Schumacher, M., S. Camp, Y. Maulet, M. Newton, K. MacPhee-Quigley, S. S. Taylor, T. Friedmann, and P. Taylor. Primary structure of *Torpedo californica* acetylcholinesterase deduced from its cDNA sequence. *Nature (Lond.)* **319**:407–409 (1986).
7. Wolfe, A. D. The monoclonal antibody AE-2 modulates fetal bovine serum acetylcholinesterase substrate hydrolysis. *Biochim. Biophys. Acta* **997**:232–235 (1989).
8. Radic, Z., E. Reiner, and P. Taylor. Role of the peripheral anionic site in acetylcholinesterase inhibition by substrates and coumarin derivatives. *Mol. Pharmacol.* **39**:98–104 (1991).
9. Purdie, J. E., and R. A. McIvor. Modification of the esteratic activity of acetylcholinesterase by alkylation with 1,1-dimethyl-2-phenylaziridinium ion. *Biochim. Biophys. Acta* **128**:590–593 (1966).
10. Bellesu, B., and V. DiTullio. Specific labelling of the curare binding sites of acetylcholinesterase and some properties of the modified enzyme. *Can. J. Biochem.* **49**:1131–1133 (1971).
11. O'Brien, R. D. Binding sites of cholinesterases. *Biochem. J.* **113**:713–719 (1969).
12. O'Brien, R. D., and K. E. Test. Exploration of the binding sites of acetylcholinesterase with protein-modifying reagents. *Arch. Biochem. Biophys.* **187**:113–120 (1978).
13. Shafferman, A., B. Velan, A. Ordenlich, C. Kronman, H. Grosfeld, M. Leitner, Y. Flashner, Y. Cohen, D. Barak, and N. Ariel. Substrate inhibition of acetylcholinesterase: residues affecting signal transduction from the surface to the catalytic center. *EMBO J.* **11**:3561–3568 (1992).
14. Sussman, J. L., M. Harel, F. Frolov, C. Offner, A. Goldman, L. Toker, and I. Silman. Atomic structure of acetylcholine-binding protein. *Science (Washington D. C.)* **253**:872–879 (1991).
15. De La Hoz, D., B. P. Doctor, J. S. Ralston, R. S. Rush, and A. D. Wolfe. A simplified procedure for the purification of large quantities of mammalian acetylcholinesterase. *Life Sci.* **39**:195–199 (1986).
16. Ellman, G. L., K. D. Courtney, V. Andres, Jr., and R. M. Featherstone. A new and rapid colorimetric determination of acetylcholinesterase activity. *Biochem. Pharmacol.* **8**:88–95 (1961).

17. Main, A. R. Affinity and phosphorylation constants for the inhibition of esterases by organophosphates. *Science (Washington D. C.)* **144**:992-993 (1964).
18. Wasserman, L., B. P. Doctor, M. K. Gentry, and P. Taylor. Epitope mapping of form specific and non-specific antibodies to acetylcholinesterase. *J. Neurosci.*, in press.
19. Soreq, H., R. Ben-Ariz, C. A. Prody, S. Seidman, A. Gnatt, L. Neville, J. Liemann-Hurwitz, E. Lev-Lehman, D. Ginzberg, Y. Lapidot-Lipeon, and H. Zukut. Molecular cloning and construction of the coding region for human acetylcholinesterase reveals a G+C-rich attenuating structure. *Proc. Natl. Acad. Sci. USA* **87**:9688-9692 (1990).
20. McGuire, M. C., C. P. Nogueira, C. F. Bartels, H. Lightstone, A. Hajra, A. F. L. van der Spek, and O. Lockridge. Identification of the structural mutation responsible for the dibucaine-resistant (atypical) variant form of human serum cholinesterase. *Proc. Natl. Acad. Sci. USA* **86**:953-957 (1989).
21. Shafferman, A., C. Kronman, Y. Flashner, M. Leitner, H. Grofeldt, A. Ordentlich, Y. Gozes, S. Cohen, N. Ariel, D. Barak, M. Harel, I. Silman, J. Sussman, and B. Velan. Mutagenesis of human acetylcholinesterase. *J. Biol. Chem.* **267**:17640-17648 (1992).
22. Weise, C., H.-J. Kreienkamp, R. Rabe, A. Pedak, A. Aaviksaar, and F. Hucho. Anionic subsites of the acetylcholinesterase from *Torpedo californica*: affinity labelling with the cationic reagent *N,N*-dimethyl-2-phenyl-aziridinium. *EMBO J.* **9**:3885-3888 (1990).
23. Kreienkamp, H.-J., C. Weise, R. Rabe, A. Aaviksaar, and F. Hucho. Anionic subites in the catalytic center of acetylcholinesterase from *Torpedo* and *cobra* venom. *Proc. Natl. Acad. Sci. USA* **88**:6117-6121 (1991).
24. Sussman, J. L., M. Harel, and I. Silman. Three dimensional structure of acetylcholinesterase, in *Multidisciplinary Approaches to Cholinesterase Functions* (A. Shafferman and B. Velan, eds.). Plenum Press, New York (1992).
25. Aldridge, W. N., and E. Reiner. *Enzyme Inhibitors as Substrates. Interaction of Esterases with Esters of Organo-phosphorous and Carbamic Acids*. North Holland, Amsterdam (1972).

Send reprint requests to: A. D. Wolfe, Division of Biochemistry, Walter Reed Army Institute of Research, Washington, DC 20307-5100.